Reconsidering Laminate Non-Symmetry

Matthew P. O'Donnell * and Paul M. Weaver †
Bristol Composites Institute (ACCIS), University of Bristol, Bristol UK, BS8 1TR

Non-symmetric laminates are commonly precluded from composite design due to perceptions of reduced performance arising from in-and out-of-plane coupling. This coupling introduces warpage during cure - leading to raised stresses, together with diminished buckling and load carrying capacity. However, these reduced performance characteristics are rarely quantified and included in the design process, instead the *"symmetric-only"* paradigm remains pervasive at the cost of a significantly reduced design space. Warpage is largely driven by mismatch in the coefficients of thermal expansion between sub-laminates located above and below the mid-plane and can be predicted by classical laminate theory. Acknowledging that all symmetric laminates in multi-part structures have build stresses from assembly, we propose that subsets of non-symmetric laminates, that translate to similar raised stress levels, be considered for design. Challenging this *"symmetric-only"* design paradigm would permit greater design freedom and offer new routes to elastically tailor composite structures. Further analysis of structural performance is assessed in terms of reduced loading and buckling capacity.

Nomenclature

$\alpha_{11,22}$	Ply coefficients of thermal expansion
$\beta_{\frac{D}{d}}$	Modified buckling parameter for reduced stiffness laminates
β_D	Buckling parameter for symmetric laminate
$\bullet_{11,22,66,12,16,26}$	Subscripts describing components of 3×3 stiffness matrices
ΔT	Change in temperature from stress-free state
ν_{12}	Poisson's ratio for ply
Ω_ε	Strain limit bounded feasible region
$\mathbf{\Gamma}$, $\mathbf{\Gamma}_{\mathrm{QI},1,2,3,4}$	Material matrices vector and components
$\mathbf{\Gamma}^{\mathrm{th}}$, $\mathbf{\Gamma}^{\mathrm{th}}_{\mathrm{QI},1,2,3,4}$	Thermal material matrices vector and components

*Lecturer in Composite Structures - Corresponding Author: Matt.ODonnell@bristol.ac.uk
†Professor in Lightweight Structures

$\boldsymbol{\kappa}$, $\kappa_{x,y,xy}$	Curvature vector and components
$\boldsymbol{\varepsilon}$, $\varepsilon_{x,y,xy}$	Mid-plane strain vector and components
$\boldsymbol{\xi}^{\mathbf{A,B,D}}$ $\xi^{\mathbf{A,B,D}}_{1,2,3,4}$	Lamination parameter vectors and components
a, **b**, **d**	Partially inverted laminate stiffness matrices
A, **B**, **D**	Laminate stiffness matrices
M, $\mathbf{M}^{\text{th}}$	Out-of-plane stress resultants mechanical and thermal
$\mathbf{M}^F$	Moment resultant required to flatten a warped plate
N, $\mathbf{N}^{\text{th}}$	In-plane stress resultants mechanical and thermal
Q	Ply stiffness matrix
E_{11}, E_{22}	Longitudinal and transverse modulus for ply
G_{12}	Shear modulus for ply
h_{ply}	Thickness of ply
$W_{1,2,3,4,5}$, $W^{\text{th}}_{1,2}$	Mechanical and thermal material invariant parameters

I. Introduction

When multi-part composite components are manufactured, or assembled post-cure, there is always some unavoidable level of build or manufacturing stress, often leading to warping. Acknowledging the existence of such residual stresses and strains, and quantifying them, opens up the possibility of design and manufacture to predetermined acceptable tolerances. As warping is, in part, due to coefficient of thermal expansion (CTE) mismatch, non-symmetry may be considered as one of many contributing factors producing defects.This alternative approach is in contrast to traditional design philosophies that often impose arbitrary, over-constraining rules that force the use of *"symmetric-only"* laminates. Other alternative sources of warpage, such as local material variability, chemical shrinkage, and tool-part interactions during cure [1], are not considered here . As manufacturing warpage is considered to be a key barrier to industrial uptake of non-symmetric laminates we focus on this aspect as the critical design driver.

Non-symmetric laminates display varying levels of warping during cure, the magnitude of which depends on the particular layup. Classical laminate theory [2] provides a robust method to capture these effects. Changing layup, leads to a range of laminate responses, from those that do not warp [3], to others that display varying degrees of warping [4]. As it is clear that not all non-symmetric layups are alike, we assert that those laminates that display modest levels of warping

be considered for design purposes, as symmetric laminates already are, based on their predicted response. We propose that the existing *"symmetric-only"* design paradigm is modified, instead allowing non-symmetric laminates that produce nominal levels of warping. These nominal levels of strain are similar in magnitude to other sources of accepted defect. Considering one such comparison, the rate of cooling can vary the observed residual strains by 5000 micro-strain [5] for a thermoplastic system and chemical shrinkage strains of a glass/polyester laminate in the longitudinal direction of approximately 400 micro-strain [6]. Our approach, therefore considers the acceptance of thermally induced warpage as one of many sources of manufacturing defect. More generally we suggest that a range of response-based metrics, for example buckling performance, could be used to guide the suitability of non-symmetry within given laminate designs. Indeed, in the context of design practice we envisage a relaxation of the hard *"symmetric-only"* constraint to be replaced with application specific response metrics, of which we propose two such examples. The expanded design space that can be achieved via a soft, response-based, approach to non-symmetry allows a remarkable increase in design freedom. Such an enhanced design space for laminate selection provides greater scope for tailoring, especially in critical areas between regions where two laminates are blended (e.g across rib bays in aircraft wing skins), including effects of ply drop-offs. In particular, the induced coupling between in-and-out of plane behaviour could be utilised for beneficial purposes in geometrically non-symmetric structures [7, 8], harnessed as a route to achieve novel structural responses [9, 10] and offer greater design freedom for impact resistance [11].

To meet ever increasing performance requirements the full potential of composites could be exploited further than current practice allows. This outcome requires existing design approaches to be challenged, in particular, to include the effects of accepting modest levels of non-symmetry. A secondary motivation for this work can be understood by considering that many structural components are geometrically non-symmetric, for example stringer stiffened panels. Geometric non-symmetry is already largely ignored due to a combination of perceived lack of significant structural effect and modelling complexity [12]. Despite industrial practice to eliminate coupling between the in-and out-of plane response, such coupling between membrane and bending response often remains in the combined plate-reinforcement region leading to unfavourable consequences, e.g. early onset stringer debonding. It follows, that when trying to achieve optimal designs, particularly in those instances where an inherent non-symmetry exists, laminates of non-symmetric stacking sequence should also be considered [10]. After all, such an approach has shown potential increases in the load carrying capacity of a stringer termination [13].

Maximising structural performance is increasingly essential in composite design. Optimal solutions are often found at the extremes of the design space. Finding the limits and, in turn, maximising the size of that design space becomes an implicit requirement for any successful optimisation. Furthermore, by allowing coupling, between in-and out-of-plane response, another mechanism through which elastic tailoring can be achieved is created. This paper seeks to highlight the restrictive nature of the existing *"symmetric-only"* design paradigm, and by challenging it, open up the potential for improved component performance.

Building on work that demonstrated some non-symmetric laminates that do not warp during cure [3, 14, 15] and more recent investigations into more general classifications of warp free laminates [16–18], an analytical modelling approach is developed, based on Classical Laminate Theory (CLT).Specifically, CLT is used to identify the warping effect of CTE mismatch exhibited by non-symmetric laminates that can be characterised by the nominal restorative strains induced by returning a thermally warped plate to its desired geometric configuration. This response thus mimics the generation of build stresses by "forcing" component plates together. The extent of the expanded design space, when compared to the symmetric-only designs, is presented identifying a significant increase in the number of potential lay-ups. By utilising an analytical model, as provided by CLT, the magnitude of the response can readily be predicted, without reliance on computationally expensive alternatives such as Finite Element Analysis (FEA). As such, our present methodology should be seen as outlining a response-based approach to non-symmetric laminates aimed at the preliminary design stage, following which a thorough manufacturing analysis could be conducted to determine exact behaviour on a case-by-case basis [19].

The structure of this paper is as follows. Section II outlines the process by which CLT is utilised to quantify CTE mismatch induced warpage, allowing the associated restoring induced strains to be defined. Different layups and stacking sequences are identified in terms of a reduced set of design variables, lamination parameters [20], that are used to identify a feasible design space for candidate layups. The details of the method used to explore the design space are presented in section III. The feasible space is first determined as a function of the restoring induced strains, identified by CLT. This process establishes viable build stresses, or strains, for laminate parts. In addition we make a provisional assessment on structural performance by considering the effects of non-symmetry on buckling performance and load carrying ability of a set of example laminates. The feasible space is determined for buckling performance in a similar manner to that of warping strains. The extent of the feasible space is then presented as a function of warping strains, buckling reduction, and load carrying capability. The exact design space for laminates of up to ten plies is discussed in section IV, allowing trends in behaviour for thicker laminates to be identified.

II. Predicting Thermal Response

As is convention, we assume that layers of a laminated composite plate are perfectly bonded to each other, and that the stiffness properties may be condensed to the mid-plane. To achieve this formulation the stresses and stiffness properties are integrated through the thickness of the plate, forming the basis of CLT [2]. The mid-plane resultants, $\mathbf{N}$ and $\mathbf{M}$ per unit length are related to the curvatures, $\boldsymbol{\kappa}$, and mid-plane strains, $\boldsymbol{\varepsilon}$, via the $\mathbf{A}$, $\mathbf{B}$, and $\mathbf{D}$ stiffness matrices,

$$\begin{bmatrix}\mathbf{N}\\ \mathbf{M}\end{bmatrix} = \begin{bmatrix}\mathbf{A} & \mathbf{B}\\ \mathbf{B} & \mathbf{D}\end{bmatrix}\begin{bmatrix}\boldsymbol{\varepsilon}\\ \boldsymbol{\kappa}\end{bmatrix}, \qquad \begin{bmatrix}\boldsymbol{\varepsilon}\\ \mathbf{M}\end{bmatrix} = \begin{bmatrix}\mathbf{a} & \mathbf{b}\\ -\mathbf{b}^{\mathrm{T}} & \mathbf{d}\end{bmatrix}\begin{bmatrix}\mathbf{N}\\ \boldsymbol{\kappa}\end{bmatrix}, \qquad \begin{bmatrix}\boldsymbol{\varepsilon}\\ \boldsymbol{\kappa}\end{bmatrix} = \begin{bmatrix}\mathbf{a}' & \mathbf{b}\mathbf{d}^{-1}\\ \mathbf{d}^{-1}\mathbf{b}^{\mathrm{T}} & \mathbf{d}^{-1}\end{bmatrix}\begin{bmatrix}\mathbf{N}\\ \mathbf{M}\end{bmatrix}, \tag{1}$$

$$\mathbf{a} = \mathbf{A}^{-1}, \qquad \mathbf{b} = -\mathbf{A}^{-1}\mathbf{B}, \qquad \mathbf{d} = \mathbf{D} - \mathbf{B}\mathbf{A}^{-1}\mathbf{B}, \qquad \mathbf{a}' = \left(\mathbf{A} - \mathbf{B}\mathbf{D}^{-1}\mathbf{B}\right)^{-1}. \tag{2}$$

The formulation can be be modified to include temperature effects, for a given change in temperature ΔT,

$$\begin{bmatrix} \mathbf{N} \\ \mathbf{M} \end{bmatrix} = \begin{bmatrix} \mathbf{A} & \mathbf{B} \\ \mathbf{B} & \mathbf{D} \end{bmatrix} \begin{bmatrix} \boldsymbol{\varepsilon} \\ \boldsymbol{\kappa} \end{bmatrix} - \Delta T \begin{bmatrix} \mathbf{N}^{th} \\ \mathbf{M}^{th} \end{bmatrix}. \tag{3}$$

The thermal resultants $\mathbf{N}^{th}$ and $\mathbf{M}^{th}$ describe the equivalent mechanical loads required to produce the same strain and curvature arising from a change in temperature from the stress free state. In this case by cooling from the cure temperature.

Lamination parameters allow the stiffness properties of a laminate to be represented in a compact way [20]. The lamination parameters can also be used to define thermal stress resultants per-Kelvin and can be calculated using the CTEs. For an N-ply laminate the summation definition of lamination parameters is,

$$\begin{aligned}
\xi_1^A &= \frac{1}{2}\sum_{i=1}^{N} \cos 2\theta_i \,(t_i - t_{i-1}), & \xi_1^B &= \frac{1}{2}\sum_{i=1}^{N} \cos 2\theta_i \left(t_i^2 - t_{i-1}^2\right), & \xi_1^D &= \frac{1}{2}\sum_{i=1}^{N} \cos 2\theta_i \left(t_i^3 - t_{i-1}^3\right), \\
\xi_2^A &= \frac{1}{2}\sum_{i=1}^{N} \cos 4\theta_i \,(t_i - t_{i-1}), & \xi_2^B &= \frac{1}{2}\sum_{i=1}^{N} \cos 4\theta_i \left(t_i^2 - t_{i-1}^2\right), & \xi_2^D &= \frac{1}{2}\sum_{i=1}^{N} \cos 4\theta_i \left(t_i^3 - t_{i-1}^3\right), \\
\xi_3^A &= \frac{1}{2}\sum_{i=1}^{N} \sin 2\theta_i \,(t_i - t_{i-1}), & \xi_3^B &= \frac{1}{2}\sum_{i=1}^{N} \sin 2\theta_i \left(t_i^2 - t_{i-1}^2\right), & \xi_3^D &= \frac{1}{2}\sum_{i=1}^{N} \sin 2\theta_i \left(t_i^3 - t_{i-1}^3\right), \\
\xi_4^A &= \frac{1}{2}\sum_{i=1}^{N} \sin 4\theta_i \,(t_i - t_{i-1}), & \xi_4^B &= \frac{1}{2}\sum_{i=1}^{N} \sin 4\theta_i \left(t_i^2 - t_{i-1}^2\right), & \xi_4^D &= \frac{1}{2}\sum_{i=1}^{N} \sin 4\theta_i \left(t_i^3 - t_{i-1}^3\right),
\end{aligned} \tag{4}$$

where θ_i and h_i are the angle and position of the i^{th} ply, and H the total thickness. The normalised positions, t_i are given by

$$t_i = 2\frac{h_i}{H}. \tag{5}$$

The lamination parameters can be thought of as integral-weighted averages of ply orientation through-the-thickness and reduces the number of ply orientation variables to an upper limit of 12. The lamination parameter vectors can then be

defined as [21],

$$\boldsymbol{\xi}^A = \begin{bmatrix} 1 \\ \xi_1^A \\ \xi_2^A \\ \xi_3^A \\ \xi_4^A \end{bmatrix}, \qquad \boldsymbol{\xi}^B = \begin{bmatrix} 0 \\ \xi_1^B \\ \xi_2^B \\ \xi_3^B \\ \xi_4^B \end{bmatrix} \qquad \boldsymbol{\xi}^D = \begin{bmatrix} 1 \\ \xi_1^D \\ \xi_2^D \\ \xi_3^D \\ \xi_4^D \end{bmatrix}, \tag{6}$$

together with the material property matrices,

$$\boldsymbol{\Gamma} = \begin{bmatrix} \boldsymbol{\Gamma}_{\mathrm{QI}} & \boldsymbol{\Gamma}_1 & \boldsymbol{\Gamma}_2 & \boldsymbol{\Gamma}_3 & \boldsymbol{\Gamma}_4 \end{bmatrix}, \tag{7}$$

defined as

$$\boldsymbol{\Gamma}_{\mathrm{QI}} = \begin{bmatrix} W_1 & W_4 & 0 \\ W_4 & W_1 & 0 \\ 0 & 0 & W_5 \end{bmatrix}, \qquad \boldsymbol{\Gamma}_1 = \begin{bmatrix} W_2 & 0 & 0 \\ 0 & -W_2 & 0 \\ 0 & 0 & 0 \end{bmatrix}, \qquad \boldsymbol{\Gamma}_2 = \begin{bmatrix} W_3 & -W_3 & 0 \\ -W_3 & W_3 & 0 \\ 0 & 0 & -W_3 \end{bmatrix},$$
$$\boldsymbol{\Gamma}_3 = \frac{1}{2}\begin{bmatrix} 0 & 0 & W_2 \\ 0 & 0 & W_2 \\ W_2 & W_2 & 0 \end{bmatrix}, \qquad \boldsymbol{\Gamma}_4 = \begin{bmatrix} 0 & 0 & W_3 \\ 0 & 0 & -W_3 \\ W_3 & -W_3 & 0 \end{bmatrix}, \tag{8}$$

with

$$\begin{aligned} W_1 &= \frac{1}{8}(3Q_{11} + 3Q_{22} + 2Q_{12} + 4Q_{66}), & W_2 &= \frac{1}{2}(Q_{11} - Q_{22}), \\ W_3 &= \frac{1}{8}(Q_{11} + Q_{22} - 2Q_{12} - 4Q_{66}), & W_4 &= \frac{1}{8}(Q_{11} + Q_{22} + 6Q_{12} - 4Q_{66}), \\ W_5 &= \frac{1}{8}(Q_{11} + Q_{22} - 2Q_{12} + 4Q_{66}), \end{aligned} \tag{9}$$

where W_i are completely described using the ply stiffnesses, Q_{ij}, and are invariant with respect to the plies orientation angle [21]. Using the Kronecker product, "$\otimes$" , and the 3×3 identity matrix, $\mathbf{I}_3$, the stiffness matrices can be described compactly as a linear combination of laminate thickness, material invariants, and layup,

$$\mathbf{A} = H\,\boldsymbol{\Gamma}\left(\boldsymbol{\xi}^A \otimes \mathbf{I}_3\right), \qquad \mathbf{B} = \frac{H^2}{4}\,\boldsymbol{\Gamma}\left(\boldsymbol{\xi}^B \otimes \mathbf{I}_3\right), \qquad \mathbf{D} = \frac{H^3}{12}\,\boldsymbol{\Gamma}\left(\boldsymbol{\xi}^D \otimes \mathbf{I}_3\right), \tag{10}$$

The thermal stress resultants per-Kelvin can be calculated using the CTEs,

$$\mathbf{N}^{th} = \frac{H}{2}\boldsymbol{\Gamma}^{\mathrm{th}}\boldsymbol{\xi}^{A}, \qquad \mathbf{M}^{th} = \frac{H^2}{8}\boldsymbol{\Gamma}^{\mathrm{th}}\boldsymbol{\xi}^{B}, \tag{11}$$

with $\boldsymbol{\Gamma}^{\mathrm{th}}$ defined similarly to that of the stiffness matrices,

$$\boldsymbol{\Gamma}^{\mathrm{th}} = \begin{bmatrix} \boldsymbol{\Gamma}^{\mathrm{th}}_{\mathrm{QI}} & \boldsymbol{\Gamma}^{\mathrm{th}}_{1} & \boldsymbol{\Gamma}^{\mathrm{th}}_{2} & \boldsymbol{\Gamma}^{\mathrm{th}}_{3} & \boldsymbol{\Gamma}^{\mathrm{th}}_{4} \end{bmatrix} \tag{12}$$

where

$$\boldsymbol{\Gamma}^{\mathrm{th}}_{\mathrm{QI}} = \begin{bmatrix} W^{\mathrm{th}}_{1} \\ W^{\mathrm{th}}_{1} \\ 0 \end{bmatrix}. \qquad \boldsymbol{\Gamma}^{\mathrm{th}}_{1} = \begin{bmatrix} W^{\mathrm{th}}_{2} \\ -W^{\mathrm{th}}_{2} \\ 0 \end{bmatrix}. \qquad \boldsymbol{\Gamma}^{\mathrm{th}}_{2,4} = \begin{bmatrix} 0 \\ 0 \\ 0 \end{bmatrix} \qquad \boldsymbol{\Gamma}^{\mathrm{th}}_{3} = \begin{bmatrix} 0 \\ 0 \\ W^{\mathrm{th}}_{2} \end{bmatrix}. \tag{13}$$

and thermal invariants $W^{\mathrm{th}}_{1,2}$ [22], where α_{ii} are the CTEs,

$$\begin{aligned} W^{\mathrm{th}}_{1} &= \alpha_{11}Q_{11} + (\alpha_{11} + \alpha_{22})\,Q_{12} + \alpha_{22}Q_{22}. \\ W^{\mathrm{th}}_{2} &= \alpha_{11}Q_{11} + (\alpha_{22} - \alpha_{11})\,Q_{12} - \alpha_{22}Q_{22}. \end{aligned} \tag{14}$$

By utilising the inverted form of equation (3) the curvature of the panel is

$$\boldsymbol{\kappa} = \mathbf{d}^{-1}\left(\mathbf{b}^{\mathrm{T}}\left(\mathbf{N} + \Delta T\,\mathbf{N}^{th}\right) + \left(\mathbf{M} + \Delta T\,\mathbf{M}^{th}\right)\right). \tag{15}$$

Assuming there are no external mechanical loads then it becomes clear that the warp-free (i.e. zero curvature) condition is

$$\mathbf{M}^{th} + \mathbf{b}^{\mathrm{T}}\mathbf{N}^{th} = \mathbf{0}. \tag{16}$$

Although $\mathbf{B} = \mathbf{0}$ ensures $\boldsymbol{\kappa} = \mathbf{0}$ it is simply sufficient, and a less restrictive condition is necessary. This result, on the necessity $\mathbf{B} = \mathbf{0}$, and examples of layups which satisfy this more general constraint have been explored in detail [3, 16].

As we are simultaneously able to consider the effect of an applied, modest, mechanical action a warped plate may be forced into a zero curvature state. The actions, $\mathbf{N}$ and $\mathbf{M}$, for the flat plate requirement are

$$\mathbf{b}^{\mathrm{T}}\mathbf{N} + \mathbf{M} = -\Delta T\,\left(\mathbf{b}^{\mathrm{T}}\mathbf{N}^{th} + \mathbf{M}^{th}\right). \tag{17}$$

As there is no restriction on the relative magnitudes of $\mathbf{N}$ and $\mathbf{M}$ it can be assumed that the restoring process is achieved by a purely moment action, providing a unique solution to (17), that is representative of a realistic physical implementation. We note that the optimal combination of actions would match the thermal stress resultants, removing all residual thermally-induced mechanical strains. As only a moment action, $\mathbf{M}^F$, is applied and the plate is in a flattened state, the through-thickness variation in strains is removed, however an additional component of in-plane strain is introduced. The additional in-plane strain attributed to this restoring action is,

$$\boldsymbol{\varepsilon} = \mathbf{bd}^{-1}\mathbf{M}^F = -\Delta T\,\mathbf{bd}^{-1}\left(\mathbf{b}^{\mathrm{T}}\mathbf{N}^{th} + \mathbf{M}^{th}\right). \tag{18}$$

We remark that this definition focuses on the restorative behaviour of flat plates, for curved structures induced strain could instead be defined relative to the change in curvatures required to return to a given desired configuration. Furthermore, where the geometric form of the structure acts to restrict deformations (e.g. example doubly curved shells) then the extent of thermal warpage reduces in comparison to a plate that is free to deform as assumed here. Using equation (18), it is possible to define a feasible region that is a function of the stiffness matrices defined by the lamination parameters, $\Omega_{\boldsymbol{\varepsilon}}\left(\boldsymbol{\xi}^A, \boldsymbol{\xi}^B, \boldsymbol{\xi}^D\right)$. The lamination parameter definition encompasses all viable stacking sequences for arbitrary numbers of plies such that the magnitude of the strains does not exceed a specified limit. Utilising strain as our warping constraint removes any dependence on laminate thickness therefore allowing consideration of laminate design space in the most general sense using this approach.

The extent of this feasible region can be quantified to give an indication of the potential increases in design freedom. While it must be noted that simply expanding the design space does not guarantee improved design, by maintaining the existing "symmetric-only" design paradigm, non-symmetric laminates that could offer improved performance are strictly prohibited, therefore no improvement can be realised. The resulting response-based design spaces, for various permissible levels of non-symmetry, are now presented.

III. Establishing the Feasible Space

The bounds of the feasible region can be determined as a function of the lamination parameters for a given allowable strain, equation (18). This section establishes the size of this region, and demonstrates that in allowing nominal strains, induced by restoring a warped plate, the design space is significantly expanded beyond that of symmetric laminates.

Obtaining a complete analytical description of the feasible regions for the lamination parameters remains an open question. Approaches utilising the convex hull of discrete angles have demonstrated success in providing an accurate approximation to the feasible region [23] but may not be entirely conservative for general laminates [24]. For specific angle sets, the design space can be described exactly [22]. As such we proceed assuming an angle set of [0, 90, ±45] thereby highlighting the effect of non-symmetry for ply angles typically used in industry. We remark that the method of

Table 1 Material Properties of IM7-8552 and curing temperature range assumed for analysis

E_{11}	163.300	GPa	T_{cure}	453	K
E_{22}	10.790	GPa	$T_{\text{post cure}}$	288	K
G_{12}	5.0	GPa	ΔT	-165	K
ν_{12}	0.288				
α_{11}	0.1×10^{-6}	1/K			
α_{22}	33.0×10^{-6}	1/K			
h ply	0.125	mm			

allowable classification herein remains equally applicable to general ply sets.

In order to capture the expanded design space we first note that by setting $\boldsymbol{\xi}^B = \mathbf{0}$ there is no warping due to non-symmetry induced CTE mismatch and, therefore, no induced warping strain. The feasible region $\Omega_{\boldsymbol{\varepsilon}}$ for $\boldsymbol{\xi}^A$ and $\boldsymbol{\xi}^D$, is therefore trivial. For this reason this investigation focuses on the $\boldsymbol{\xi}^B$ region. The vector, $\boldsymbol{\xi}^B$, is generally defined by four variable components, but reduces to three for the proposed angle set since $\xi_4^B = 0$ for all laminates.

The representative material utilised is IM7-8552 whose properties can be found in Table 1 together with the temperature difference, ΔT, assumed in our analysis. These values may differ slightly from the standard industrial values [25] and and are taken from extensive characterisation tests [26].

A. Allowable Strains

In order to determine the extent of the feasible space, a series of lamination parameters direction vectors were generated. The components represent the nine variable components of $\boldsymbol{\xi}^A$, $\boldsymbol{\xi}^B$, and $\boldsymbol{\xi}^D$. These vectors were chosen to lie in one half of a nine-dimensional hyper-sphere bounding the combined $\xi_{1,2,3}^{A,B,D}$ space. A total of 50,000 vectors were analysed as a combination of pre-defined directions and additional randomly selected directions. The pre-defined directions are those aligned with each of the 9 lamination parameter axes, and all diagonal permutations of these axes. This approach ensures a direction vector is generated in the direction of each vertex of the nine-dimensional hyper-cube that bounds the lamination parameter space and the centre point of each bounding hyper-plane. As the direction vector lies outside of the feasible domain a series of 101 *"anisotropic scale factors"* (ASFs), in the range $[-1, 1]$, are applied thereby reducing the magnitude of the direction vector and determining the relative magnitude of each of the lamination parameters. Each point generated along the direction vector has its feasibility assessed via the established lamination parameter constraints [22]. All points that are considered feasible are subsequently analysed to determine their physical response. The ASF provides a basic metric for capturing how the stiffness matrices deviate from an equivalent quasi-isotropic system composed of the same material. Changes in the magnitude of the ASF capture deviation in the stiffness matrices from $\boldsymbol{\Gamma}_{\mathbf{QI}}$, as defined by equation (10). When the ASF is zero, by definition all lamination parameters are equivalently zero, corresponding to the quasi-isotropic laminate. As the ASF's magnitude is increased so do the lamination parameters, this introduces contributions from $\boldsymbol{\Gamma}_{\mathbf{1-4}}$ leading to anisotropic behaviour.

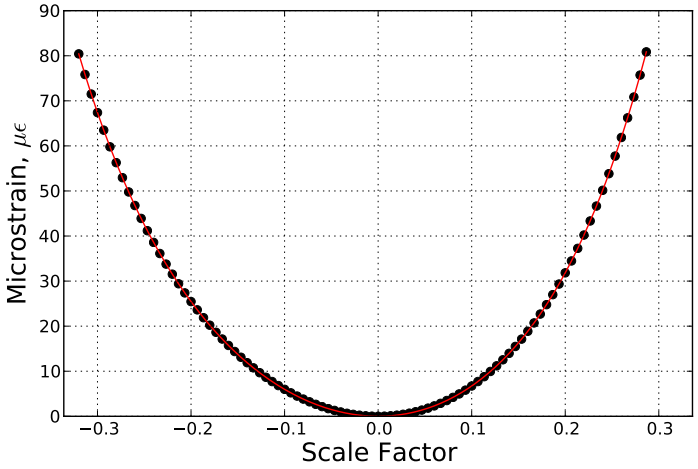

Fig. 1 Typical test vector's relationship between ASF and restoring strain - continuous 10^{th} order polynomial fit (red line) and sampled points (black circles)

The relationship between ASF and restoring strain is calculated for each lamination parameter vector satisfying the angle set's feasibility constraints. The discrete sampling points can be represented by a 10^{th} order polynomial fit in order to obtain a continuous profile, figure 1. Although a more physically representative function could have been selected this approach ensures a successful fit for all lamination parameter vectors. For a given strain limit the maximum and minimum ASF can be found. The convex hull of the collection of points described by the lamination parameter vector, scaled by the ASF, is used to describe the feasible space, $\Omega_{\boldsymbol{\varepsilon}}$. The convex hull of these points, for a given strain limit, represents the best approximation to the true feasible space for a given number of points*.

Examples of the feasible space are shown for an allowed restoring induced strain of 10, 50, and 100 microstrain, Figures 2a–2c. These plots represent just three dimensions of the total nine-dimensional space. It is interesting to note that all of the warp-free non-symmetric configurations previously identified [16], lie on the line defined by $\xi_1^B = \xi_3^B = 0$, indicating the collapse of the space for zero strain allowable.

B. Buckling Reduction

The coupling stiffness matrix terms, **B**, can introduce an unfavourable reduction in the buckling capacity of components. This is, in part, due to the notional reduction of effective bending stiffness from **D** to **d**, where $\mathbf{d} = \mathbf{D} - \mathbf{B}\mathbf{A}^{-1}\mathbf{B}$, equation (2). As buckling is often a driving design constraint, we seek to quantify the negative effects of non-symmetry, whilst demonstrating that viable non-symmetric designs still exist. Such design practice changes must be seen as part of the holistic paradigm change to response-based symmetry requirements, therefore, allowing the extraction of maximum performance. As buckling is a complex phenomenon, dependent on geometry, loading, and boundary conditions, an indicative measure of this effect is required.

*If a more accurate representation is required the number of trial vectors could be increased beyond 50,000 used herein.

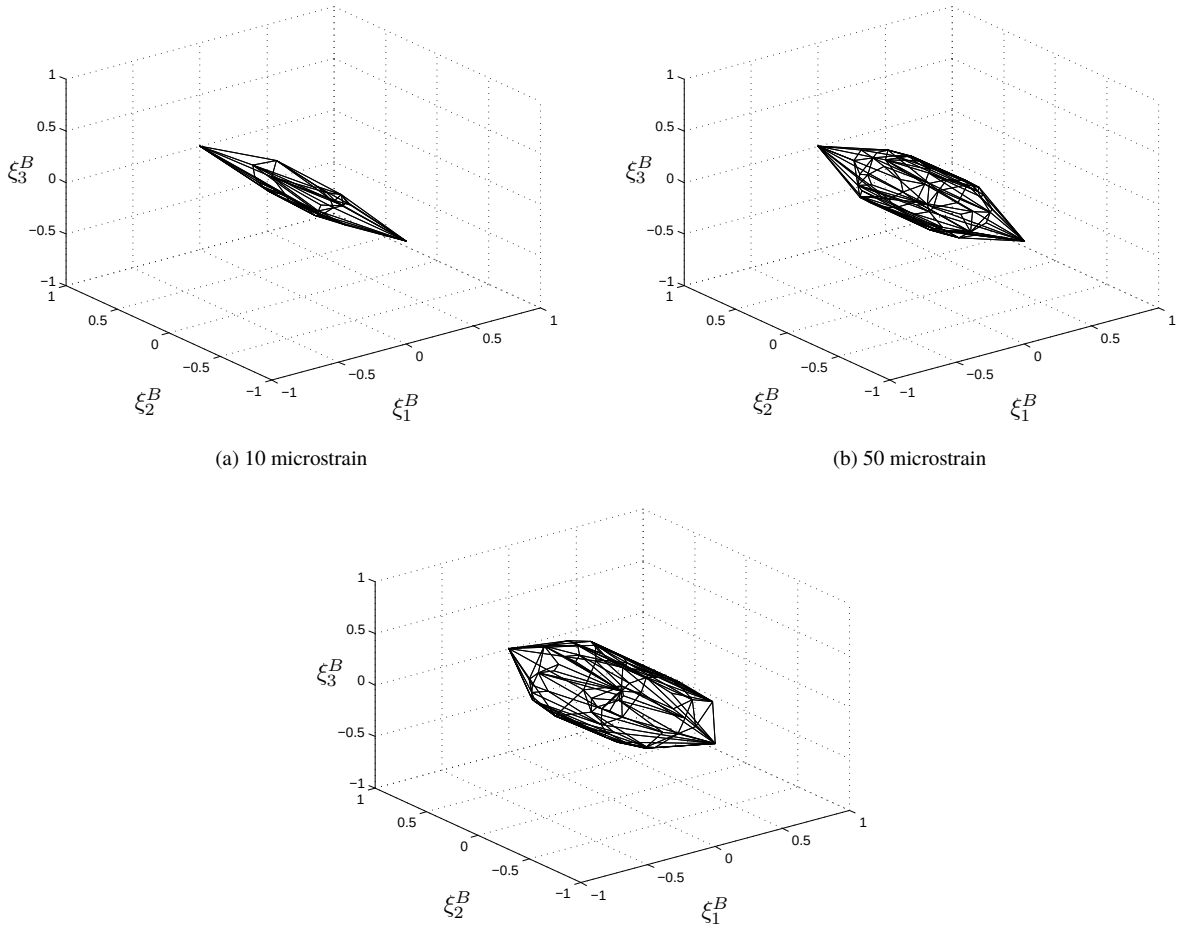

(a) 10 microstrain

(b) 50 microstrain

(c) 100 microstrain

Fig. 2 Feasible space for $\xi^{\mathbf{B}}$ for increasing restoring strains

The validity of a buckling analysis has been questioned when considering non-symmetric laminates of cross-ply configurations [27]. In particular, it is often thought that out-of-plane deformation due to coupling occurs upon the onset of loading, suggesting buckling may not occur in all cases, depending on the severity of coupling. However, this phenomenon is not always an accurate reflection of behaviour, in reality its dependence on the type of loading and boundary conditions has been established [28–30]. Finding a suitable analytical buckling constraint to capture all effects of non-symmetry on buckling is a complex problem, and beyond the scope of this current work. As an example of one of the many possible response-based metrics we introduce a parameter that captures a notional percentage knockdown associated with the use of the reduced bending stiffness **d** instead of bending stiffness **D**. Our metric provides a simple estimate of the order of magnitude reduction in buckling load. We proceed by considering the non-dimensional parameter, β_D, that can be used to evaluate the buckling capacity of flat plates subject to combined loading, including compression and shear [29],

$$\beta_D = \frac{\mathrm{D}_{12} + 2\mathrm{D}_{66}}{\mathrm{D}_{11}\mathrm{D}_{22}}. \tag{19}$$

For laminates with non-symmetry the bending capacity is often represented via the reduced stiffness matrix. As bending stiffness is always reduced by **B** coupling, it would be beneficial to quantify this effect on buckling via analytical formulation. It is prudent to note, that utilising the reduced stiffness matrix can be considered a conservative predictor of buckling capacity as any beneficial effects of load redistribution are neglected. To simplify analysis and gauge the extent of any possible reduction the following ratio is proposed as a simple metric,

$$\beta_{\frac{d}{D}} = \frac{\mathrm{d}_{12} + 2\mathrm{d}_{66}}{\mathrm{D}_{12} + 2\mathrm{D}_{66}}, \tag{20}$$

based on the numerator properties of β_D and equivalent values for β_d.

This measure does not capture all effects of non-symmetry on buckling behaviour. The decision to capture the reduction using the numerator of equation (19) was made to highlight the difference between **D** and **d**. While this is not the only ratio of stiffness properties that could have been proposed it is representative of the underlying mechanics of the buckling coefficient by including the relationships between **D**, **B**, and **d**. This indicator allows illustrative trends to be observed - noting that exact prediction of buckling loads is unnecessary at this stage. In the design and optimisation of actual components, warping, buckling, and load carrying ability, together with any other performance indicators could be included. By allowing appropriately constrained non-symmetry an optimisation procedure would have the potential to select both non and fully symmetric designs as the constraints dictated.

Following a similar process to that outlined in section III.A for finding the boundary of the warping strain limited feasible space the relationship between ASF and the buckling parameter $\beta_{\frac{d}{D}}$ can be observed, as shown in figure 3. The

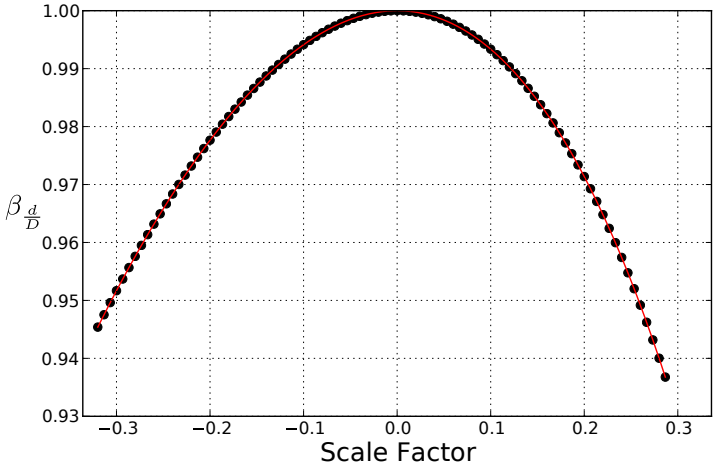

Fig. 3 Typical test vector's relationship between ASF and reduction in buckling performance - continuous 10^{th} order polynomial fit (red line) and sampled points (black circles)

convex hulls, defining the feasible region for the combined strain and buckling requirements can be calculated. The effect of the additional buckling constraint is observed in Figures 4a–4c. Imposing a limit on the reduction of buckling capacity of no more than 5%, the feasible space initially increases monotonically with the restoring strain allowable. However, as the space reaches a certain threshold of non-symmetry, the dominating factor becomes buckling reduction and the expansion is curtailed, see figure 5. A quantitative analysis of this effect is now discussed utilising the volume of the feasible space.

C. Volume of the Feasible Space

It is possible to quantify the effect of increasing the allowable restoring strain, and permitted buckling capacity reduction, by considering the volume of the associated convex hull. As the convex hull defines the bounds of the feasible region, the volume contained by this region can be considered as a basic measure of design freedom. An increase in volume is therefore associated with an increase in the design space. By tracking the change in volume, the rate of expansion as a function of both constraints can be observed. Furthermore, a larger volume is associated with larger permissible ASF and therefore greater deviation from the quasi-isotropic design, in essence a bigger volume permits more non-symmetry. By utilising volume as a metric in this manner, the continuous design space can be presented representing laminates composed of an arbitrary number of plies.

Figure 6 demonstrates that even a modest allowable strain increases the potential design space significantly. It also indicates that, above a certain feasible threshold it is the reduced stiffness properties, and therefore the reduction in buckling capacity, that determines the space's boundary. For the range of restoring strains presented in figure 6 the observed buckling reduction does not exceed 30%. This curve is therefore coincident with the case where no buckling constraint is applied. In fact, it is observed that the majority of the design space is obtained with a buckling reduction

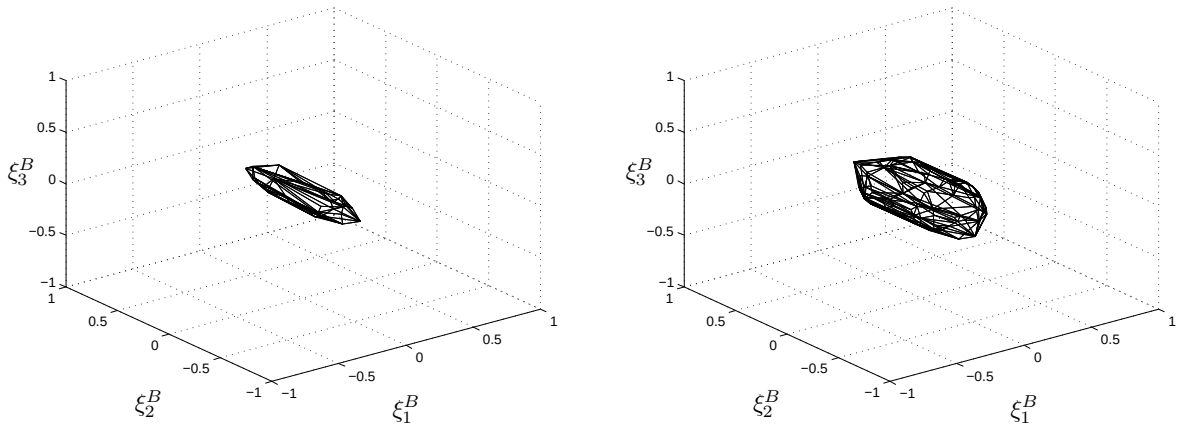

(a) 10 microstrain

(b) 50 microstrain

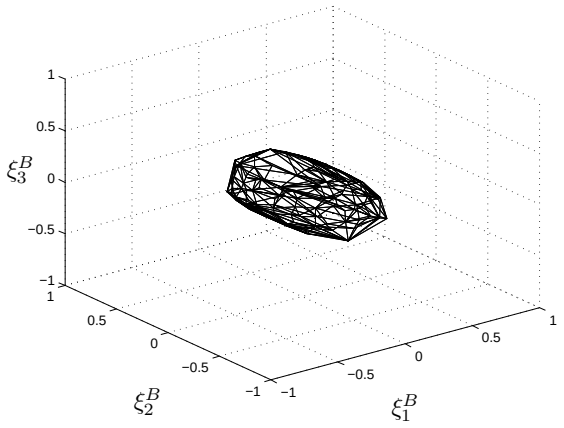

(c) 100 microstrain

Fig. 4 Feasible space for $\boldsymbol{\xi}^{\mathbf{B}}$ for increasing restoring strains with a buckling reduction $\beta_{\frac{d}{D}} \leq 5\%$

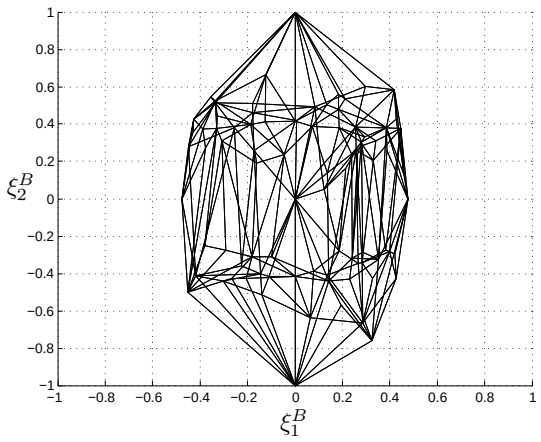

(a) No buckling constraint

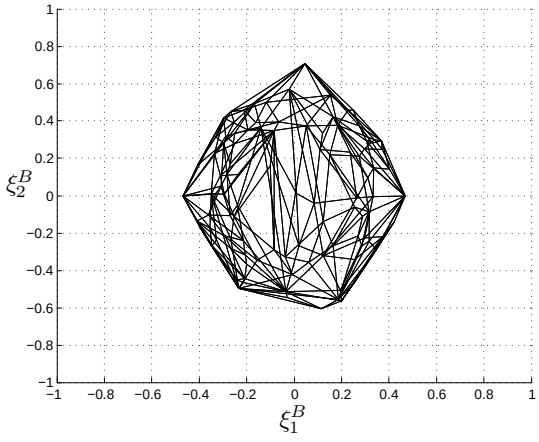

(b) Buckling reduction $\beta_{\frac{d}{D}} \leq 5\%$

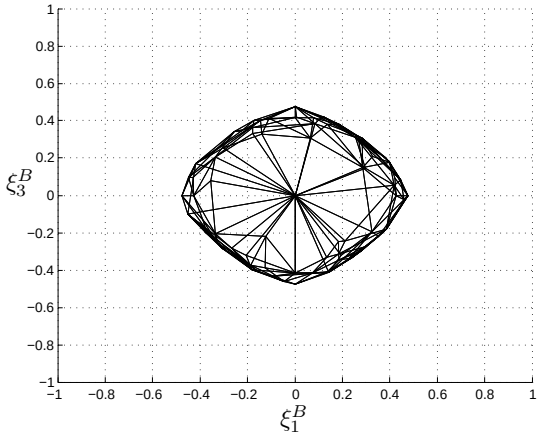

(c) No buckling constraint

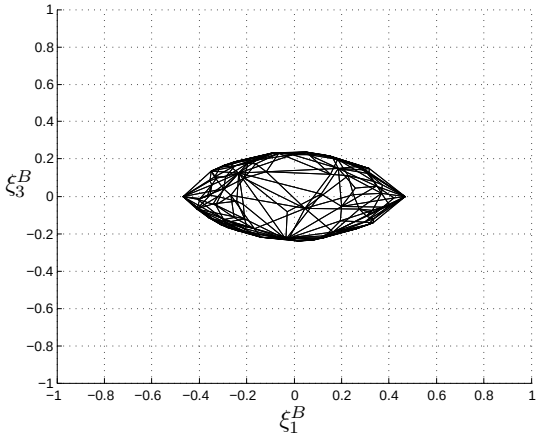

(d) Buckling reduction $\beta_{\frac{d}{D}} \leq 5\%$

Fig. 5 Effect of buckling reduction constraint on the extent of the feasible space with 100 microstrain restoring tolerance

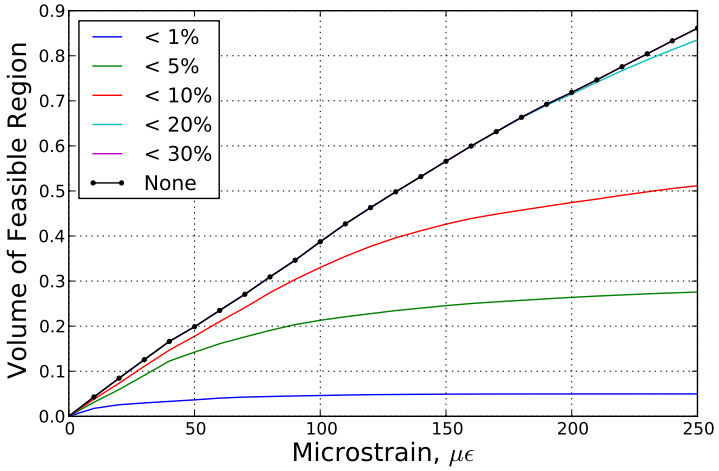

Fig. 6 Extent of the feasible space determined by convex hull's volume for a given restoring strain tolerance. Each curve represents maximum permissible reduction in buckling performance $\beta_{\frac{d}{D}}$ and the case where no bucking constraint is imposed. The no buckling constraint is coincident with the 30% reduction constraint for the range of permissible strain values shown.

not exceeding 20% at strains below 250 microstrain.

IV. Increased Available Layups

In the previous section the extent of the design space was characterised as a function of lamination parameters for limits on permissible warping strains and reduction in buckling capacity. The increase in the design space was identified by the changing volume of the feasible region. In this section we consider the exact design space for laminates of up to 10 plies, in doing so trends exhibited for thicker laminates can be observed. Table 2 indicates the number of laminates displaying symmetric layups and special cases possessing sub-symmetries - having a non-symmetric layup but zero warping as predicted by CLT [16]. We note that the total number of laminates is halved in order to avoid analysing a laminate and its reverse. An example of an eight ply laminate possessing sub-symmetry is,

$$[\theta_a,\ \theta_b,\ \theta_b,\ \theta_a,\ \theta_b,\ \theta_a,\ \theta_a,\ \theta_b] \tag{21}$$

where θ_a and θ_b are two different ply angle orientations. Further examples of laminates possessing sub-symmetry that remain warp free during cure can be found in Weaver (2005) [16]. The total design space for laminates that require restoring strains below 10 and 100 microstrain, with no limit on buckling reduction, can be compared to the results obtained for those with a buckling reduction of no more than 1, 5, or 10% in table 2. As illustrative examples the following laminates are presented to identify laminates that are non-symmetric but possess modest or zero thermal response. Each of the examples illustrate how non-symmetry as a binary exclusion criteria is

not reflective of the underlying mechanics of the system. These three examples can be contrasted with the fourth example, a laminate that maximises the thermal warping showing that a response-based design criteria is more appropriate.

- Example 1: Sub-symmetric - Non-symmetric laminate with zero **B** coupling due to matched stiffness above and below the mid-plane:

$$\begin{bmatrix} 45 & -45 & -45 & 45 & -45 & 45 & 45 & -45 \end{bmatrix}$$

$$\boldsymbol{\kappa} = \begin{bmatrix} 0 \\ 0 \\ 0 \end{bmatrix} [1/\text{m}], \qquad \mathbf{M}^F = \begin{bmatrix} 0 \\ 0 \\ 0 \end{bmatrix} [\text{Nm}], \qquad \text{abs}(\boldsymbol{\varepsilon}) = \begin{bmatrix} 0 \\ 0 \\ 0 \end{bmatrix}, \qquad \beta_{\frac{d}{D}} = 1,$$

with

$$\mathbf{A} = \begin{bmatrix} 50.3 & 40.3 & 0 \\ 40.3 & 50.3 & 0 \\ 0 & 0 & 42.1 \end{bmatrix}_{\times 10^6} [\text{N/m}], \quad \mathbf{B} = \begin{bmatrix} 0 & 0 & 0 \\ 0 & 0 & 0 \\ 0 & 0 & 0 \end{bmatrix} [\text{N}], \quad \mathbf{D} = \begin{bmatrix} 4.19 & 3.35 & 0 \\ 3.35 & 4.19 & 0 \\ 0 & 0 & 3.51 \end{bmatrix} [\text{Nm}].$$

- Example 2: Centrally non-symmetric - non-zero **B** coupling, but non-symmetric pairs located close to the mid-plane to minimise the stiffness mismatch:

$$\begin{bmatrix} 45 & 0 & 90 & 90 & 0 & 90 & 0 & 45 \end{bmatrix},$$

$$\boldsymbol{\kappa} = \begin{bmatrix} -1.38 \\ 2.39 \\ -0.85 \end{bmatrix}_{\times 10^{-3}} [1/\text{m}], \qquad \mathbf{M}^F = \begin{bmatrix} -0.966 \\ 0.966 \\ 0 \end{bmatrix} [\text{Nm}], \qquad \text{abs}(\boldsymbol{\varepsilon}) = \begin{bmatrix} 3.26 \\ 6.31 \\ 6.42 \end{bmatrix}_{\times 10^{-6}}, \qquad \beta_{\frac{d}{D}} = 0.9997,$$

with

$$\mathbf{A} = \begin{bmatrix} 78.1 & 12.4 & 9.57 \\ 12.4 & 78.1 & 9.57 \\ 9.57 & 9.57 & 14.3 \end{bmatrix}_{\times 10^6} [\text{N/m}], \quad \mathbf{B} = \begin{bmatrix} 1.20 & 0 & 0 \\ 0 & -1.20 & 0 \\ 0 & 0 & 0 \end{bmatrix}_{\times 10^3} [\text{N}], \quad \mathbf{D} = \begin{bmatrix} 6.69 & 2.05 & 1.84 \\ 2.05 & 4.30 & 1.84 \\ 1.84 & 1.84 & 2.21 \end{bmatrix} [\text{Nm}].$$

- Example 3: Counterbalanced non-symmetry - non-zero **B** coupling but with paired groups of non-symmetry used to balance the effect of non-symmetry. This could also be considered as a partially sub-symmetric laminate.

$$\begin{bmatrix} -45 & 0 & 0 & 90 & 90 & 0 & -45 & 0 \end{bmatrix},$$

$$\boldsymbol{\kappa} = \begin{bmatrix} -1.10 \\ 0.67 \\ -1.60 \end{bmatrix}_{\times 10^{-3}} [1/\mathrm{m}], \qquad \mathbf{M}^F = \begin{bmatrix} -1.14 \\ 0.352 \\ -0.364 \end{bmatrix} [\mathrm{Nm}], \qquad \mathrm{abs}(\boldsymbol{\varepsilon}) = \begin{bmatrix} 5.17 \\ 0.30 \\ 4.13 \end{bmatrix}_{\times 10^{-6}}, \qquad \beta_{\frac{d}{D}} = 0.9861,$$

with

$$\mathbf{A} = \begin{bmatrix} 97.2 & 12.4 & -9.57 \\ 12.4 & 59.0 & -9.57 \\ -9.57 & -9.57 & 14.3 \end{bmatrix}_{\times 10^{6}} [\mathrm{N/m}], \quad \mathbf{B} = \begin{bmatrix} 1.78 & -0.58 & 0.60 \\ -0.58 & -0.62 & 0.60 \\ 0.60 & 0.60 & -0.58 \end{bmatrix}_{\times 10^{3}} [\mathrm{N}], \quad \mathbf{D} = \begin{bmatrix} 9.32 & 1.61 & -1.40 \\ 1.61 & 2.54 & -1.40 \\ -1.40 & -1.40 & 1.77 \end{bmatrix} [\mathrm{Nm}].$$

- Example 4: Maximally non-symmetric - Laminate displays the maximum mismatch in stiffness above and below the mid-plane.

$$\begin{bmatrix} 0 & 0 & 0 & 0 & 90 & 90 & 90 & 90 \end{bmatrix},$$

$$\boldsymbol{\kappa} = \begin{bmatrix} 27.0 \\ 27.0 \\ 0 \end{bmatrix}_{\times 10^{-3}} [1/\mathrm{m}], \qquad \mathbf{M}^F = \begin{bmatrix} 13.3 \\ 13.3 \\ 0 \end{bmatrix} [\mathrm{Nm}], \qquad \mathrm{abs}(\boldsymbol{\varepsilon}) = \begin{bmatrix} 942 \\ 942 \\ 0 \end{bmatrix}_{\times 10^{-6}}, \qquad \beta_{\frac{d}{D}} = 0.8629,$$

with

$$\mathbf{A} = \begin{bmatrix} 87.4 & 3.13 & 0 \\ 3.13 & 87.4 & 0 \\ 0 & 0 & 5.00 \end{bmatrix}_{\times 10^{6}} [\mathrm{N/m}] \qquad \mathbf{B} = \begin{bmatrix} -19.1 & 0 & 0 \\ 0 & 19.1 & 0 \\ 0 & 0 & 0 \end{bmatrix}_{\times 10^{3}} [\mathrm{N}] \qquad \mathbf{D} = \begin{bmatrix} 7.28 & 0.26 & 0 \\ 0.26 & 7.28 & 0 \\ 0 & 0 & 0.42 \end{bmatrix} [\mathrm{Nm}]$$

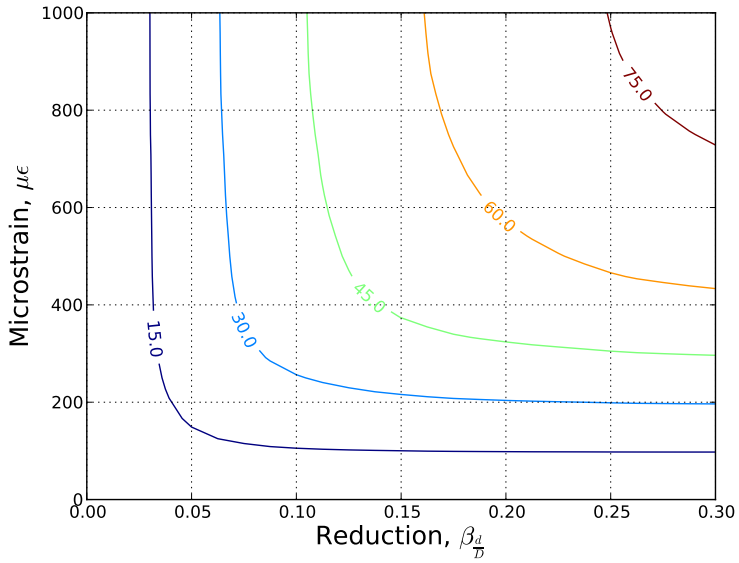

Fig. 7 Contours indicating the percentage of the total design space available for combined constraints of allowed warping strain and maximal buckling reduction - figure illustrates behaviour for laminates of 10 plies.

Considering the trends observed in the number of available laminates in table 2 it is apparent that imposing "symmetric-only" design rules significantly reduces the number of laminate configurations available. For laminates composed of 10 plies, symmetric layups represent less than 0.2% of the total design space. Even for a modest warping strain limit of 10 microstrain, and strict limit on buckling reduction, $\beta_{\frac{d}{D}}$ of 1%, the permissible design space rises to 1.9% of the total number of laminates, an almost ten-fold increase. This effect is compounded as the number of plies in a laminate increases.

An alternative representation of the data in table 2 is presented in figure 7 where the contours represent the percentage of the total design space that can be achieved for given buckling reduction and strain limits. Figure 7 demonstrates that a simultaneous increase in allowable strain and permissible buckling reduction must occur in order to continue expanding the design space. This observation reflects the results for lamination parameters shown in figure 6. The necessity for some buckling reduction, due to reduced bending stiffness (changing from **D** to **d**) illustrates that non-symmetric laminates in structures sensitive to buckling loads must be carefully considered. However, as laminates exhibit varying levels of buckling reduction, following the same argument as induced restoring strains, non-symmetric laminates should not be unnecessarily excluded from the design space.

V. Conclusions

The number of potential layups available to a designer greatly increases, as a percentage of the total design space, when viable non-symmetric laminates are considered in additional to conventional symmetric laminates. This effect

Table 2 Total number of layups for laminates of up to 10 plies possessing, symmetry, sub-symmetry, and those exhibiting restoring strains $\varepsilon_{tol} \leq$ 10 and 100 microstrain. Permissible warped layups are subdivide to include restrictions on buckling capacity reduction $\beta_{\frac{d}{D}} \leq$ 1%, 5% and 10% allowing comparison with no buckling constraint applied - None.

Number of plies, n	Total layups $4^n/2$	Symmetric	Sub Symmetric	$\varepsilon_{tol} \leq$ 10 microstrain					$\varepsilon_{tol} \leq$ 100 microstrain				
				$\beta_{\frac{d}{D}}$	None	$\leq$ 1%	$\leq$ 5%	$\leq$ 10%	$\beta_{\frac{d}{D}}$	None	$\leq$ 1%	$\leq$ 5%	$\leq$ 10%
2	8	4	0		0	0	0	0		0	0	0	0
3	32	16	0		0	0	0	0		0	0	0	0
4	128	16	0		0	0	0	0		6	0	1	1
5	512	64	0		0	0	0	0		62	0	24	46
6	2048	64	0		42	26	42	42		442	60	193	286
7	8192	256	24		162	30	150	154		1748	138	772	1124
8	32768	256	6		1040	519	960	1032		9752	1117	4332	6568
9	131072	1024	216		4238	1982	3818	4138		47364	4466	20258	32004
10	524288	1024	96		20600	10062	19294	20164		222134	21568	96900	152826

is increasingly evident as the number of plies in a laminate increases. By reconsidering non-symmetric laminates can greatly help in overconstrained designs, such as those involving ply drop offs and blending of neighbouring plate elements in multi-part structure. Prohibiting their use ultimately restricts the designer and may incur unnecessary weight penalties. The rationale against their usage is, in part, the perceived manufacturing limitations associated with thermal warping during cure due to CTE mismatch. While it has been demonstrated previously that certain sub-sets of non-symmetric laminates do not warp, our current investigation has extended this concept to plates that warp to a nominal, acceptable, limit. As the nature of non-symmetry introduces varying degrees of CTE mismatch not all plates warp to the same extent. Accepting this difference in response, and by allowing small build-induced strains, the design space is significantly increased, and with it, the potential for optimal designs. The effects of in- and out-of-plane coupling on the buckling performance have also been investigated, demonstrating that viable non-symmetric laminates remain, even when additional constraints are imposed. We assert, from these results, that a response-based approach to non-symmetry, rather than prohibition, is preferable when seeking to optimise structural performance.

The extent of this observed increase in design space has been highlighted, both through lamination parameters and explicitly via laminates of up to ten plies. Unlike symmetric laminates, that for an increased number of plies become a smaller fraction of the total design space, the number of non-symmetric laminates available that possess a nominal restoring strain increases with ply count. This observation is a significant result - offering greater design freedom.

Acknowledgements

Matthew P. O'Donnell would like to thank the Engineering and Physical Sciences Research Council (EPSRC) and Airbus UK Ltd. for their financial support during the investigation.

Data Archival

The data necessary to support the conclusions are included in the paper.

References

[1] Potter, K., "Understanding the Origins of Defects and Variability in Composites Manufacture," *International Conference on Composite Materials (ICCM)-17, Edinburgh, UK*, 2009.

[2] Mansfield, E. H., *The Bending and Stretching of Plates*, The Bending and Stretching of Plates, Cambridge University Press, 2005.

[3] Bartholomew, P., "Ply stacking sequences for laminated plates having in-plane and bending orthotropy," *Fibre Science and Technology*, Vol. 10, No. 4, 1977, pp. 239 – 253. doi:https://doi.org/10.1016/0015-0568(77)90001-X, URL http://www.sciencedirect.com/science/article/pii/001505687790001X.

[4] Weaver, P. M., O'Donnell, M. P., and York, C., "Approximations for Warp-Free Laminate Configurations," *51st AIAA/ASME/ASCE/AHS/ASC Structures, Structural Dynamics, and Materials Conference*, 2010. doi:10.2514/6.2010-2774, URL https://arc.aiaa.org/doi/abs/10.2514/6.2010-2774.

[5] Tsukada, T., ichi Takeda, S., Minakuchi, S., Iwahori, Y., and Takeda, N., "Evaluation of the influence of cooling rate on residual strain development in unidirectional carbon fibre/polyphenylenesulfide laminates using embedded fibre Bragg grating sensors," *Journal of Composite Materials*, Vol. 51, No. 13, 2017, pp. 1849–1859. doi:10.1177/0021998316662327, URL https://doi.org/10.1177/0021998316662327.

[6] Bogetti, T. A., and John W. Gillespie, J., "Process-Induced Stress and Deformation in Thick-Section Thermoset Composite Laminates," *Journal of Composite Materials*, Vol. 26, No. 5, 1992, pp. 626–660. doi:10.1177/002199839202600502, URL https://doi.org/10.1177/002199839202600502.

[7] Fletcher, T. A., Butler, R., and Dodwell, T. J., "Anti-symmetric laminates for improved consolidation and reduced warp of tapered C-sections," *Advanced Manufacturing: Polymer & Composites Science*, Vol. 1, No. 2, 2015, pp. 105–111. doi:10.1179/2055035914Y.0000000010, URL https://doi.org/10.1179/2055035914Y.0000000010.

[8] Minera Rebulla, S., Patni, M., Weaver, P. M., Pirrera, A., and O'Donnell, M. P., "Comparing the effect of geometry and stiffness on the effective load paths in non-symmetric laminates," *AIAA SCITECH 2019, San Diego California, 7-11 January*, American Institute of Aeronautics and Astronautics Inc. (AIAA), United States, 2019. doi:10.2514/6.2019-1766, URL https://arc.aiaa.org/doi/abs/10.2514/6.2019-1766.

[9] Stacey, J., O'Donnell, M., and Schenk, M., "Thermal Prestress in Composite Compliant Shell Mechanisms," *Journal of Mechanisms and Robotics*, Vol. 11, No. 2, 2019. doi:10.1115/1.4042476.

[10] O'Donnell, M. P., Stacey, J. P., Chenchiah, I. V., and Pirrera, A., "Multiscale tailoring of helical lattice systems for bespoke thermoelasticity," *Journal of the Mechanics and Physics of Solids*, Vol. 133, 2019, p. 103704. doi:10.1016/j.jmps.2019.103704.

[11] Baker, N., Butler, R., and York, C. B., "Damage tolerance of fully orthotropic laminates in compression," *Composites Science and Technology*, Vol. 72, No. 10, 2012, pp. 1083 – 1089. doi:https://doi.org/10.1016/j.compscitech.2011.09.010, URL http://www.sciencedirect.com/science/article/pii/S026635381100337X, recent Advancements in Deformation & Fracture of Composites: Experiment & Analysis.

[12] Kassapoglou, C., *Design and Analysis of Composite Structures: With Applications to Aerospace Structures*, Aerospace Series, John Wiley & Sons, 2011.

[13] O'Donnell, M. P., Weaver, P. M., and Cosentino, E., "Debond Resisting Composite Stringers," *53rd AIAA/ASME/ASCE/AHS/ASC Structures, Structural Dynamics and Materials Conference*, Honolulu, Hawaii, 2012. doi:10.2514/6.2012-1613, URL https://arc.aiaa.org/doi/abs/10.2514/6.2012-1613.

[14] Caprino, G., and Visconti, I. C., "A Note On Specially Orthotropic Laminates," *Journal of Composite Materials*, Vol. 16, No. SEP, 1982, pp. 395–399. doi:10.1177/002199838201600504, URL https://doi.org/10.1177/002199838201600504.

[15] Gunnink, J. W., "A Note On Specially Orthotropic Laminates - Comment," *Journal of Composite Materials*, Vol. 17, No. 6, 1983, pp. 508–510. doi:10.1177/002199838301700603, URL https://doi.org/10.1177/002199838301700603.

[16] Weaver, P. M., "Anisotropic Laminates that Resist Warping during Manufacture," *ICCM15 - 15th International Conference on Composite Materials*, Durban, South Africa, 2005.

[17] York, C. B., "Characterization of non-symmetric forms of fully orthotropic laminates," *Journal of Aircraft*, Vol. 46, No. 4, 2009, pp. 1114–1125. URL https://doi.org/10.2514/1.32938.

[18] Vannucci, P., "General Theory of Coupled Thermally Stable Anisotropic Laminates," *Journal of Elasticity*, Vol. 113, No. 2, 2013, pp. 147–166. doi:10.1007/s10659-012-9415-0, URL https://doi.org/10.1007/s10659-012-9415-0.

[19] Baran, I., Cinar, K., Ersoy, N., Akkerman, R., and Hattel, J. H., "A Review on the Mechanical Modeling of Composite Manufacturing Processes," *Archives of Computational Methods in Engineering*, Vol. 24, No. 2, 2017, pp. 365–395. doi: 10.1007/s11831-016-9167-2, URL https://doi.org/10.1007/s11831-016-9167-2.

[20] Tsai, S. W., Halpin, J. C., and Pagano, N. J., "Composite Materials Workshop," *Proceedings of the summer workshop: Physical aspects of composite materials held at Washington University, St. Louis, Mo. 1967, sponsered by the ONR-ARPA Association of Monsanto and Washington University.*, Technomic, Westport CT, 1968, pp. 233–253.

[21] Gürdal, Z., Haftka, R. T., and Hajela, P., *Design and Optimization of Laminated Composite Materials*, Wiley-Interscience publication, Wiley, 1999.

[22] Diaconu, C. G., and Sekine, H., "Layup Optimisation for Buckling of Laminated Composite Shells with Restricted Layer Angles," *AIAA journal*, Vol. 42, No. 10, 2004, pp. 2153–2163. doi:10.2514/1.931, URL https://doi.org/10.2514/1.931.

[23] Bloomfield, M. W., Diaconu, C. G., and Weaver, P. M., "On feasible regions of lamination parameters for lay-up optimization of laminated composites," *Proceedings of the Royal Society A: Mathematical, Physical and Engineering Science*, Vol. 465, No. 2104, 2009, pp. 1123–1143. doi:10.1098/rspa.2008.0380, URL https://royalsocietypublishing.org/doi/abs/10.1098/rspa.2008.0380.

[24] Wu, Z., Raju, G., and Weaver, P. M., "Framework for the Buckling Optimization of Variable-Angle Tow Composite Plates," *AIAA Journal*, Vol. 53, No. 12, 2015, pp. 3788–3804. doi:10.2514/1.J054029, URL https://doi.org/10.2514/1.J054029.

[25] Hexcel, "Material Data Repository," http://www.hexcel.com/, 2012. Accessed: 10/02/2012.

[26] Panesar, A. S., "Multistable Morphing Composites Using Variable Angle Tows (VAT)," PhD dissertation, University of Bristol, Department of Aerospace Engineering, 2012.

[27] Qatu, M. S., and Leissa, A. W., "Buckling or Transverse Deflections of Unsymmetrically Laminated Plates Subjected to In-Plane Loads," *AIAA Journal*, Vol. 31, No. 1, 1993, pp. 189–194. doi:10.2514/3.11336, URL https://doi.org/10.2514/3.11336.

[28] Diaconu, C. G., and Weaver, P. M., "Postbuckling of long unsymmetrically laminated composite plates under axial compression," *International Journal of Solids and Structures*, Vol. 43, No. 22, 2006, pp. 6978 – 6997. doi:https://doi.org/10.1016/j.ijsolstr.2006.02.017, URL http://www.sciencedirect.com/science/article/pii/S0020768306000497.

[29] Weaver, P. M., "Approximate analysis for buclking of compression loaded long rectangular plates with flexural/twist anisotropy," *Proceedings of the Royal Society A.*, Vol. 462, 2006, pp. 59–73. doi:10.1098/rspa.2005.1552, URL https://royalsocietypublishing.org/doi/abs/10.1098/rspa.2005.1552.

[30] Weaver, P. M., and Nemeth, M. P., "Bounds on Flexural Properties and Buckling Response for Symmetrically Laminated Composite Plates," *ASCE, Journal of Engineering Mechanics*, Vol. 133, No. 11, 2007, pp. 1178–1191. doi:10.1061/(ASCE)0733-9399(2007)133:11(1178), URL https://ascelibrary.org/doi/abs/10.1061/%28ASCE%290733-9399%282007%29133%3A11%281178%29.